Effects of noise on lidar data inversion with the backward algorithm

Adolfo Comerón, Francesc Rocadenbosch, Miguel Angel López, Alejandro Rodríguez, Constantino Muñoz, David García-Vizcaíno, and Michaël Sicard

The lidar data–inversion algorithm widely known as the Klett method (and its more elaborate variants) has long been used to invert elastic-lidar data obtained from atmospheric sounding systems. The Klett backward algorithm has also been shown to be robust in the face of uncertainties concerning the boundary condition. Nevertheless electrical noise at the photoreceiver output unavoidably has an impact on the data-inversion process, and describing in an explicit way how it affects retrieval of the atmospheric optical coefficients can contribute to improvement in inversion quality. We examine formally the way noise disturbs backscatter-coefficient retrievals done with the Klett backward algorithm, derive a mathematical expression for the retrieved backscatter coefficient in the presence of noise affecting the signal, and assess the noise impact and suggest ways to limit it.

OCIS codes: 280.0280, 280.3640, 120.0280.

1. Introduction

The most extended method for inverting data from monostatic, monochromatic, and single-scattering lidar systems are what is known currently as the Klett backward algorithm and its variants.[1,2] These methods eliminate the need for knowledge of the lidar system constant in exchange for knowledge of a boundary condition (usually the value of the backscatter coefficient at the maximum range of the inversion[3]) and provide robustness in the face of noise and uncertainties in knowledge of the boundary condition.[1,4] With the Klett backward algorithm[1] the atmosphere backscatter coefficient β as a function of the range R is retrieved from the values of received power:

$$\beta(R) = \frac{\beta_m R^2 P(R)}{R_m{}^2 P(R_m) + 2\beta_m \int_R^{R_m} \frac{z^2 P(z)}{C(z)}\,\mathrm{d}z}, \qquad (1)$$

where $P(R)$ is the power received from range R, R_m is the maximum range, $\beta_m = \beta(R_m)$ is the boundary condition, and $C(R) = \beta(R)/\alpha(R)$ is the (in principle range-dependent) ratio between the backscatter coefficient and the extinction coefficient α. In general we cannot expect to determine $C(R)$ until $\alpha(R)$ is determined, since it is in fact part of the solution. We are not concerned with this problem here; it has been discussed by Klett.[5]

Therefore, if we assume that $C(R)$ is known, uncertainties in the retrieval of β depend only on the boundary condition β_m. This suggests that the inversion should be started from a range R_m where the signal-to-noise ratio is high enough and β_m is known to a good degree of approximation. The condition of a signal-to-noise ratio that is high enough may, however, be difficult to achieve in some practical cases, especially when one is working at long wavelengths where the Rayleigh scattering is low and photoreceivers based on photomultiplier tubes may not be practical. In those cases one may be led to start the inversion at ranges for which the received power estimate coming from the photoreceiver output is highly contaminated by noise, which affects backscatter-coefficient retrieval. Although the effects of misestimated values of β_m have been completely quantified,[4,6–8] and the effect of noise has been addressed through numerical simulation by Klett,[1] a formal expression quantifying the noise effects seems not to have been presented so far. Such an expression is derived in Section 2. Its implications are discussed in Section 3. In view of the results in

The authors are with the Photonics Laboratory, Electromagnetics and Photonics Engineering Group, Department of Signal Theory and Communications, Universitat Politècnica de Catalunya, Campus Nord UPC, Jordi Girona 1-3, 08034 Barcelona, Spain. (e-mail for A. Comerón, comeron@tsc.upc.es).

Received 18 July 2003; revised manuscript received 10 December 2003; accepted 30 January 2004.

0003-6935/04/122572-06$15.00/0

Section 3, the methods—customarily used by lidarists on an empirical basis—through which the noise impact can be diminished is critically examined in Section 4. Through inversion of real lidar data, the big impact that noise affecting the signal coming from the farthest distance in the inversion range can have and the reduction of that impact that can be achieved through proper noise averaging are illustrated in Section 5. The concluding remarks in Section 6 summarize the contributions.

2. Retrieval in the Presence of Noise

In a general real situation the photoreceiver output is proportional to

$$\hat{P}(R) = P(R) + n(R), \tag{2}$$

where $n(R)$ represents the instantaneous "power noise" affecting the measurement at range R. Note that, by subtracting the bias terms from the signal at the output of the photoreciever, $n(R)$ can be made a zero-mean process that can therefore have positive and negative values. This is assumed throughout this paper. The magnitude retrieved is then $\hat{\beta}(R)$, which, according to algorithm (1), is computed as

$$\frac{1}{\hat{\beta}(R)} = \frac{1}{R^2\hat{P}(R)}\left[\frac{1}{\beta_m}R_m{}^2\hat{P}(R_m) + 2\int_R^{R_m}\frac{z^2\hat{P}(z)}{C(z)}\,dz\right]. \tag{3}$$

Substituting Eq. (2) into Eq. (3) leads, after some straightforward algebraic manipulations, to

$$\frac{1}{\hat{\beta}(R)} = \left[\frac{1}{\beta(R)} + \frac{1}{\beta_m}\frac{R_m{}^2 n(R_m)}{R^2P(R)} + \frac{2}{R^2P(R)}\int_R^{R_m}\frac{z^2n(z)}{C(z)}\,dz\right]\frac{P(R)}{P(R)+n(R)}. \tag{4}$$

In Eq. (4) one can recognize an "instantaneous" noise effect in the factor $P(R)/[P(R) + n(R)]$ as well as a "memory" noise effect containing both the effect of noise in the cell at R_m where the inversion is started and the cumulative effect of the noise along the inversion path:

$$m(R) = \frac{1}{\beta_m}\frac{R_m{}^2 n(R_m)}{R^2P(R)} + \frac{2}{R^2P(R)}\int_R^{R_m}\frac{z^2n(z)}{C(z)}\,dz. \tag{5}$$

Using the above definition for $m(R)$, we can rewrite the retrieved backscatter coefficient given by Eq. (4) as

$$\hat{\beta}(R) = \left[1 + \frac{n(R)}{P(R)}\right]\frac{\beta(R)}{1 + m(R)\beta(R)}. \tag{6}$$

3. Impact of the Different Noise Terms

It is clear that the

$$\left[1 + \frac{n(R)}{P(R)}\right]$$

factor in Eq. (6) produces a ripple proportional to the inverse of the signal-to-noise ratio in the retrieved backscatter coefficient. Taking into account Eq. (5), the noise cumulative effect, represented by the term $m(R)\beta(R)$ in the denominator of Eq. (6), which in addition to a ripple in general produces a bias, can be split into two components:

$$\beta(R)m(R) = \zeta_m(R) + \zeta_i(R) \tag{7}$$

with

$$\zeta_m(R) = \frac{\beta(R)}{\beta_m}\frac{R_m{}^2 n(R_m)}{R^2P(R)} \tag{8a}$$

containing the effect of the noise at the maximum range of the inversion and

$$\zeta_i(R) = 2\beta(R)R_m\frac{R_m{}^2\int_{R/R_m}^1 \xi^2\frac{n_n(\xi)}{C_n(\xi)}\,d\xi}{R^2P(R)}, \tag{8b}$$

with $n_n(\xi) = n(R_m\xi)$ and $C_n(\xi) = C(R_m\xi)$, including the integrated effect of noise along the retrieval path.

Equation (8a) shows that picking up a particular resolution cell greatly affected by noise to start the inversion may have an important impact in the inversion because the value of the noise in that cell is multiplied by $R_m{}^2$. From the practical point of view it underscores the importance of averaging the noise-affected signal over a number of cells around the one from which the inversion is to be started and of assigning the resulting value of the average to this cell, to average out the noise, as discussed below.

Although the effect of noise on a specific inversion in general depends on noise realization [for example, if $n(R_m)$ happens to be zero in a specific case, $\zeta_m(R)$ given by Eq. (8a) will have no effect in that particular case], an idea of the relative importance of Eqs. (8a) and (8b) can be obtained from their rms values.

It is clear that the rms value of Eq. (8a) is

$$\langle\zeta_m\rangle^{1/2} = \frac{\beta(R)}{\beta_m}\frac{R_m{}^2\sigma_{nm}}{R^2P(R)}, \tag{9}$$

with σ_{nm} the noise rms value at range R_m.

The mean squared value of Eq. (8b) can be written in turn as

$$\langle\zeta_i{}^2(R)\rangle = \frac{4\beta^2(R)R_m{}^6}{R^4P^2(R)}\int_{R/R_m}^1\int_{R/R_m}^1 \times\frac{\xi_1{}^2\xi_2{}^2}{C_n(\xi_1)C_n(\xi_2)}\,r_{\xi nn}(\xi_1, \xi_2)d\xi_1d\xi_2, \tag{10}$$

where $r_{\xi nn}(\xi_1, \xi_2) = \langle n_n(\xi_1, \xi_2)\rangle$ is the autocorrelation function of $n_n(R/R_m)$.

An upper bound to Eq. (10) can be calculated assuming that the noises in different resolution cells are uncorrelated. This is a reasonable approximation if $\Delta\tau \geq 1/(2B)$, where $\Delta\tau$ is the sampling period of the acquisition system and B is the photoreceiver bandwidth. In these conditions the spatial autocorrelation function for the noise can be approximated as

$$r_{znn}(z_1, z_2) = \sigma_n{}^2(z_1)\Delta R\delta(z_1 - z_2), \qquad (11)$$

where ΔR is the system range resolution and $\delta(z)$ is Dirac's delta function; the dependence of σ_n on the range takes into account the possibility that signal-induced shot noise is significant. Then $r_{\xi nn}(\xi_1, \xi_2) = [(\Delta R)/R_m]\sigma_n{}^2(R_m\xi_1)\delta(\xi_1 - \xi_2)$ and

$$\langle \zeta_i{}^2(R)\rangle^{1/2} < \frac{2\beta(R)R_m}{C_{\min}}\left\{\frac{1}{5}\frac{\Delta R}{R_m} \times \left[1 - \left(\frac{R}{R_m}\right)^5\right]\right\}^{1/2} \frac{R_m{}^2\sigma_{n\,\max}(R)}{R^2P(R)}, \qquad (12)$$

where $C_{\min}$ is the minimum value of $C(R)$ in the inversion range and $\sigma_{n\,\max}(R)$ is the maximum value of σ_n within the range (R, R_m).

4. Reduction of the Noise Effect

Equation (9) and expression (12) are compared with 1. According to the lidar equation,

$$R^2P(R) = A\beta(R)\exp[-2\int_0^R \alpha(x)\mathrm{d}x], \qquad (13)$$

where A is the system constant (range-dependent overlap effects are disregarded), leading to

$$\langle \zeta_m{}^2(R)\rangle^{1/2} = \frac{\sigma_{nm}}{P(R_m)}\exp[-2\int_R^{R_m} \alpha(x)\mathrm{d}x]. \qquad (14)$$

Equation (14) shows that the effect of the noise in the cell from which the inversion is started tends to decrease as the range R becomes shorter. However, for optically thin atmospheres $\langle \zeta_m{}^2(R)\rangle^{1/2}$ is virtually independent of R, and, if no particular care is taken as to the choice of the data sample from which the inversion is started, an important bias may occur at any range if the signal-to-noise ratio at R_m is small.

The effect of the $\zeta_m(R)$ term can be reduced by proper choice of the inversion starting point, i.e., by choosing a resolution cell where the noise realization is small. Assuming that $P(R)$ varies slowly around R_m, the reduction of the noise effect in the starting cell can be achieved by averaging the values of $\hat{P}(R)$ over a number of resolution cells around R_m and forcing $\hat{P}(R_m)$ to this average value. Calling N the number of cells over which the averaging is carried out, this operation divides by $\sqrt{N}$ the effective value of σ_{nm} appearing in Eq. (9). Equation (2) shows that the maximum allowable value of N is determined by the dependence of the received power on R being well

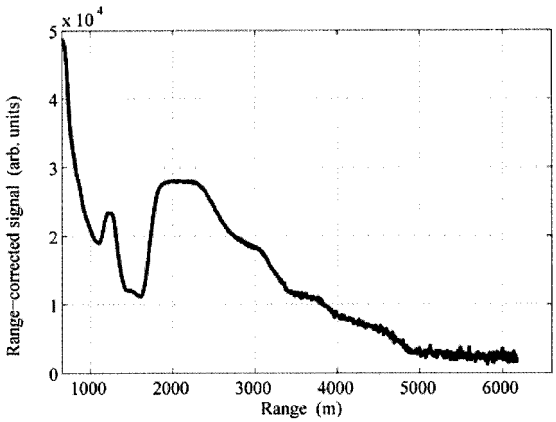

Fig. 1. Lidar range-corrected signal between 600 and 6180 m for 4000 pulses integrated at 1064 nm.

approximated by a linear law through the range covered by the N cells, in which case the averaged power value coincides well with the value at range R_m. In a zone dominated by molecular scattering the linear-law approximation will be safely satisfied with a maximum N given by the condition $N\Delta R \approx 200$ m.

The relative influence of the terms ζ_m and ζ_i can be assessed by dividing expression (12) by Eq. (9), which yields

$$\frac{\langle \zeta_i{}^2(R)\rangle^{1/2}}{\langle \zeta_m{}^2(R)\rangle^{1/2}} < \frac{2R_m\beta_m\sqrt{N}}{C_{\min}}\frac{\sigma_{n\,\max}(R)}{\sigma_{nm}} \times \left\{\frac{1}{5}\frac{\Delta R}{R_m}\left[1 - \left(\frac{R}{R_m}\right)^5\right]\right\}^{1/2}, \qquad (15)$$

where the possibility of averaging $\hat{P}(R_m)$ over N cells around R_m has been taken into account. The form of expression (15) shows that the effect of the cumulative noise effect tends to be small compared with the effect of the noise in the cell at R_m for values of R close

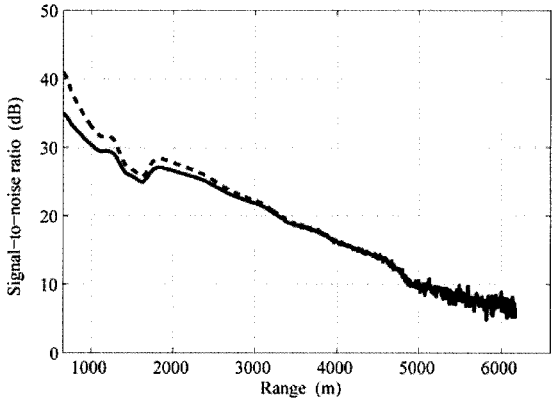

Fig. 2. Estimate of the signal-to-noise ratio for the example lidar signal being studied. The discontinuous line takes into account only photoreceiver noise and background-radiation shot noise. The continuous curve also shows the effect of the signal-induced shot noise.

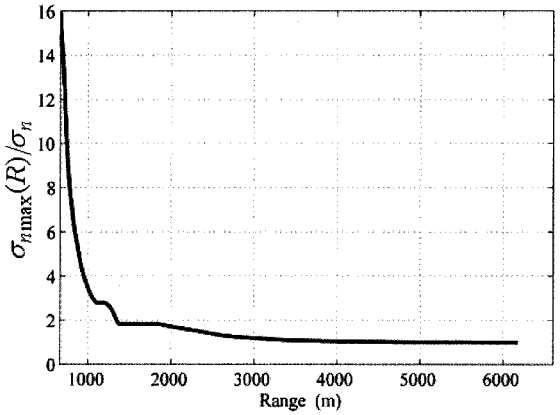

Fig. 3. Estimate of the ratio $[\sigma_{n\ \max}(R)]/\sigma_{nm}$ for the lidar-signal example being studied.

to R_m because of the factor $1 - (R/R_m)^5$ in the square root. The factor

$$\frac{2R_m\beta_m}{C_{\min}}\sqrt{\frac{1}{5}\frac{\Delta R}{R_m}}$$

is likely to be smaller than 1. For example, assuming that $\beta_m = 10^{-5}$ m^{-1} sr^{-1}, which is a high backscatter-coefficient value in practice for the near IR and the visible, $C_{\min} = 0.01$ sr^{-1}, $R_m = 10000$ m, and $\Delta R = 7.5$ m, we have

$$\frac{2R_m\beta_m}{C_{\min}}\left(\frac{1}{5}\frac{\Delta R}{R_m}\right)^{1/2} = 0.24.$$

In most situations of practical interest, with vertical or slant paths, β_m will be much smaller than the value just assumed, tending to further decrease the ratio

$$\frac{\langle\zeta_i^{\,2}(R)\rangle^{1/2}}{\langle\zeta_m^{\,2}(R)\rangle^{1/2}}.$$

As to the ratio $[\sigma_{n\ \max}(R)]/\sigma_{nm}$ in expression (15), its value falls between values set by the two limiting cases, namely, noise limited by the photoreceiver and noise limited by the signal. In the former case, noise is independent of the signal, thus of the range, and $\sigma_{n\ \max} = \sigma_{nm}$. In the latter both σ_{nm} and $\sigma_{n\ \max}$ are proportional to the square root of the signal (at R_m

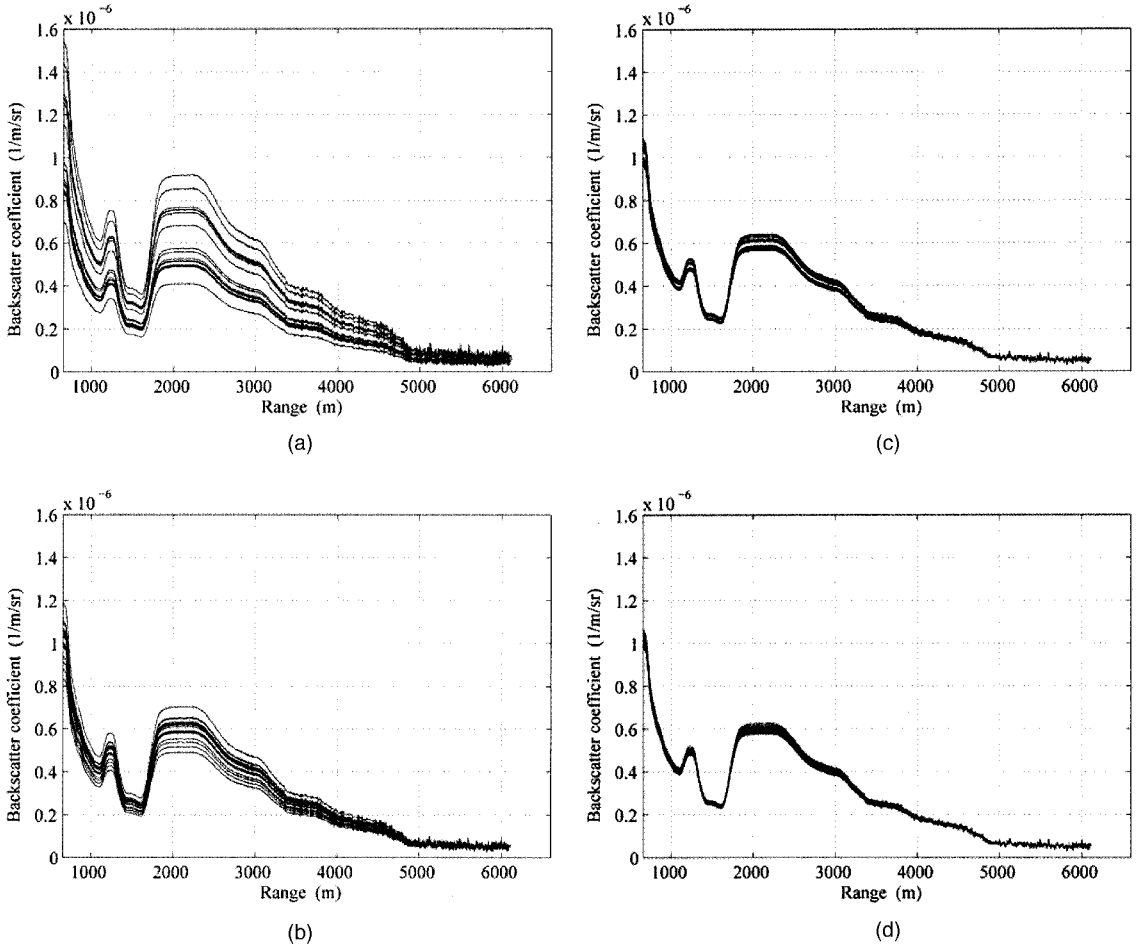

Fig. 4. Backscatter coefficient inversions starting from $R_m = 6000$ to $R_m = 6120$ m. (a) $\hat{P}(R_m)$ is taken directly as the value contained in the resolution cell corresponding to R_m. (b) $\hat{P}(R_m)$ is taken as the average of R_m and the $R_m \pm 7.5$ m cells ($N = 3$ cells). (c) $\hat{P}(R_m)$ is taken as the average of the cells between $R_m - 30$ and $R_m + 30$ m ($N = 9$ cells). (d) $\hat{P}(R_m)$ is taken as the average of the cells between $R_m - 60$ and $R_m + 60$ m ($N = 17$ cells).

and at the range where $\sigma_{n\,\max}$ occurs, respectively), so that $(\sigma_{n\,\max})/\sigma_{nm}$ is half of the signal dynamic range between R and R_m. For receivers based on avalanche photodiodes (APD's) $\sigma_n(R)$ is likely to be determined by the photoreceiver for most of the measurement range, and only for distances closest to the lidar is the signal-induced shot noise noticeable.

For a given receiver and measurement conditions, reducing ΔR does not decrease $\langle \zeta_i^{\,2} \rangle^{1/2}$ because the receiver bandwidth must increase accordingly, and, if the noise spectrum is flat, the product $(\Delta R)^{1/2}\sigma_{n\,\max}$ in Eq. (12) remains constant. This means that, for a given range resolution, the only way of lessening $\langle \zeta_i^{\,2} \rangle^{1/2}$ is by averaging a number of returns, which divides the effective noise rms value by the square root of that number. Also, the decrease in expression (15) achieved by reducing ΔR would be made at the expense of increasing $\langle \zeta_m^{\,2} \rangle^{1/2}$.

With the typical values of the atmosphere and lidar parameters, the bound given by expression (15) is expected to be much smaller than 1 for most measurement situations of practical interest, indicating that the main influence of noise in the inversion is in general the bias represented by the term ζ_m defined in Eq. (8a).

5. Example with Live Data

The effects discussed above are illustrated by the inversion of lidar live data. The data have been obtained with a transportable lidar designed, built, and operated by the Lidar Group of the Department of Signal Theory and Communications' Electromagnetics and Photonics Engineering Group at the Technical University of Catalonia [Universitat Politècnica de Catalunya (UPC), Barcelona, Spain]. In the lidar a frequency-doubled Nd:YAG laser operating at 1064 and 532 nm is used. The laser delivers pulses of ~160 mJ and 6-ns duration at both wavelengths with a 20-Hz pulse repetition frequency. The backscattered radiation is collected by a 20-cm-aperture telescope. The photoreceiver is based on a 3-mm active area APD. The electrical bandwidth is 10 MHz, and the output is digitized at 20 Msample/s, yielding a range resolution $\Delta R = 7.5$ m. The data presented here correspond to the 1064-nm wavelength, selected by placing an interference optical bandpass filter in front of the APD. At this wavelength the photoreceiver noise equivalent power, including the effect of the background radiation during the measurement, is approximately 10^{-13} W/Hz$^{1/2}$. The noise-excess factor of the APD is assumed to be 5 and its quantum efficiency 77%.

Figure 1 shows the noise-contaminated lidar range-corrected signal $\hat{S}(R) = \hat{P}(R)R^2$ between 600 and 6180 m along a 54°-elevation line of sight for a specific atmospheric situation, obtained by integrating approximately 4000 pulses. Figure 2 shows the estimated signal-to-noise ratio as a function of range. The signal-to-noise ratio exceeds a comfortable 10-dB value until the range is around 5000 m and is only around 7 dB at 6000 m. Figure 3 shows the estimated ratio $[\sigma_{n\,\max}(R)]/\sigma_{\rm nm}$.

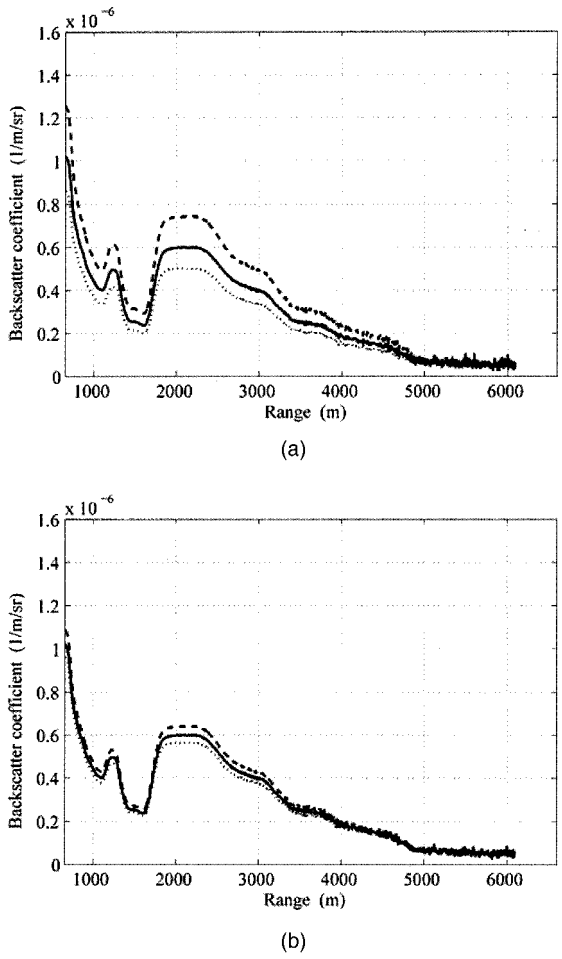

Fig. 5. Estimated 68% confidence interval, dotted curves, for the inverted backscatter coefficient: (a) $N = 1$, (b) $N = 17$.

Figure 4 shows the result of the inversion according to Eq. (1), assuming that $\beta_m = 10^{-9}\ \mathrm{m^{-1}\,sr^{-1}}$ at $R_m = 6000$ m, and a constant value $C(R) = 1/17\ \mathrm{sr^{-1}}$ for the backscatter-to-extinction ratio along the path. Note, however, that we are not emphasizing the physical characteristics of the atmosphere for this particular case [whether the chosen boundary value β_m and the backscatter-to-extinction ratio $C(R)$ accurately correspond to the actual situation] but rather the mathematical aspects of the effect of noise on the inversion. The panels in Fig. 4 show a family of 17 curves obtained as R_m moves from 6000 to 6120 m in steps of 7.5 m (the system range resolution), which should have a negligible effect on the inversion if the signal is not affected by noise. However, because the noise realization is different for the different cells, we obtain very different values for the inverted backscatter coefficient, with differences greater than 100% in case the value of the data sample $\hat{P}(R_m)$ is directly used for the different R_m[$N = 1$, Fig. 4(a)]. In Fig. 4(b), 4(c), and 4(d) $\hat{P}(R)$ is averaged over R_m and $N - 1$ adjacent cells with N having values of 3, 9, and 17, respectively; the value obtained is assigned to $\hat{P}(R_m)$. It is clear that the 17 different inversions

collapse to a narrower interval of values for each range as the averaging increases and that the narrower intervals tend to be contained within the wider ones. This is the result of the effective reduction of the noise variance in Eq. (9) discussed in Section 4. Note that when the averaging increases the families of curves tend also to exhibit decreased variability because there are less completely independent noise averages.

Note as well that, with the present system's range resolution, the value taken for R_m, the assumed boundary condition β_m, and the assumed backscatter-to-extinction ratio, expression (15) is always much smaller than 1 for all the values of N considered, so that the prevailing cause of bias in the inversion is the term defined by Eq. (8a) in this case. Assuming that the central curve $\beta_c(R)$ in Fig. 4(d) is a reliable estimate for $\beta(R)$, the intervals for a given confidence level of the inverted backscatter coefficient can be estimated by drawing curves $\beta_c(R)/[1 \pm p\langle\zeta_m{}^2(R)\rangle^{1/2}]$. Assuming Gaussian noise, the intervals for the confidence level 68% ($p = 1$) are represented for $N = 1$ [Fig. 5(a)] and for $N = 17$ [Fig. 5(b)].

6. Conclusions

A general expression has been derived for the backscatter coefficient inverted through the Klett formula from lidar measurements affected by noise. The expression allows us to identify in a formal way the noise impact. It shows an instantaneous noise effect, producing a ripple proportional to the inverse of the signal-to-noise ratio in the retrieved backscatter coefficient, and a memory effect, containing both the effect of the noise in the resolution cell where the inversion is started and the cumulative effect from the inversion starting cell to the actual point at which the backscatter coefficient is evaluated. Quantitative expressions for assessing the importance of the error that the memory effect can produce have been derived. Usually the effect of noise in the inversion-starting cell is dominant and can produce an important bias at all ranges if the signal-to-noise ratio at the farthest range is relatively small and the atmosphere optically thin. Filtering the noise through spatial averaging of the signal contaminated with noise over the cells adjacent to the one at the farthest range provides a means to reduce this effect without sacrificing spatial resolution in the inversion. This has been illustrated through a live example along a slanted line of sight.

This research was made possible by the authors' participation in the following projects: "A European Aerosol Research Lidar Network to Establish an Aerosol Climatology: EARLINET," contract EVR1-CT-1999-40003, supported by the European Commission under the Fifth Framework Programme for Research, Technological Development and Demonstration; the Spanish Ministry for Science and Technology (MCYT) project REN2000-1754-C02; project "Integració Metodològica i de Models per a la Previsió i Anàlisi de la Contaminació i el Temps i els seus Efectes" (IMMPACTE); Catalan for "Integration of Methods and Models for the Forecast and Analysis of Pollution, Weather and their Effects," funded by the Department of Environment (DMA) and the Interdepartment Commission for Research and Technological Innovation (CIRIT) of the Catalonia Autonomous Government.

The authors are indebted to Ravil R. Agishev for fruitful discussions on photoreceiver noise and to Alfredo Cano, who contributed technical skills to our compact, transportable lidar that performs reliable measurements.

References

1. J. D. Klett, "Stable analytical inversion solution for processing lidar returns," Appl. Opt. **20,** 211–220 (1981).
2. F. G. Fernald, "Analysis of atmospheric lidar observations: some comments," Appl. Opt. **23,** 652–653 (1984).
3. L. R. Bissonnette, "Sensitivity analysis of lidar inversion algorithms," Appl. Opt. **25,** 2122–2125 (1986).
4. F. Rocadenbosch and A. Comerón, "Error analysis for the lidar backward inversion algorithm," Appl. Opt. **38,** 4461–4474 (1999).
5. J. D. Klett, "Lidar inversion with variable backscatter/extinction ratios," Appl. Opt. **24,** 1638–1643 (1985).
6. Y. Sasano and H. Nakane, "Significance of the extinction/backscatter ratio and the boundary value term in the solution for the two-component lidar equation," Appl. Opt. **23,** 11–13 (1984).
7. Q. Jinhuan, "Sensitivity of lidar equation solution to boundary values and determination of the values," Adv. Atmos. Sci. **5,** 229–241 (1988).
8. M. Matsumoto and N. Takeuchi, "Effects of misestimated far-end boundary values on two common lidar inversion solutions," Appl. Opt. **33,** 6451–6456 (1994).